Supporting Information

Risner et al. 10.1073/pnas.1714888115

SI Methods

DBA/2J Mice. We obtained DBA/2J mice (3 and 10 mo, male) from the Jackson Laboratories. Animals were maintained in a 12-h light/dark cycle with standard rodent chow and water available ad libitum.

Isolating AMPA-Mediated Responses. We measured the voltage-clamped (−65 mV) AMPA receptor-mediated response to light and to AMPA (100 μM; Sigma-Aldrich) dissolved in normal Ames' medium and delivered to the cell body via a puff pipette using a controlled pneumatic system (20 psi, 20 ms duration, Picospritzer II; General Valve Co.). For these recordings, the extracellular solution included pharmacological agents to block voltage-gated Na^+ channels (tetrodotoxin, 1 μM; Tocris), $GABA_A$ receptors (picrotoxin, 50 μM; Sigma-Aldrich), glycine receptors (strychnine, 1 μM; Sigma-Aldrich), and NMDA receptors (AP5, 50 μM; Abcam). To confirm isolation of AMPA-derived current, we added CNQX (50–100 μM; Abcam) in the extracellular solution to block all AMPA/kainate receptors for comparison.

Quantification of Immunolabeling. Following perfusion of separate mouse cohorts, we prepared frozen sections through retinas of both eyes after either 2 or 4 wk of unilateral microbead-induced elevations in IOP. We labeled these sections using the following primary antibodies: anti-PSD95 (1:200; Alomone Labs), anti-RIBEYE (1:100; BD Transduction Laboratories), anti-NaV1.6 (1:200; Alomone Labs), and anti-ChAT (1:100; Millipore). For PSD95 immunostaining, sections were pretreated with 10 mM sodium citrate pH 6.0 90 °C for 30 min. Other procedures were as previously described (1). We used identical microscope settings to acquire confocal images of microbead vs. saline retinas and quantified signal in the synaptic layers by subtracting the background intensity followed by normalization with ChAT signal, which did not depend on IOP. We analyzed and averaged 2–4 images per sample. In whole retinas harvested from additional mice after 2 or 4 wk of IOP elevation, we used ImageJ to quantify NaV1.6 in RGC bodies and axons identified using antibodies against Brn3a (1:200; Santa Cruz Biotechnology) or SMI32 (1:1,000), respectively. We obtained 2–4 stacks of confocal micrographs through individual planes (60×) for each of 3–5 retinas in each experimental group. We quantified intensity of NaV1.6 in RGC bodies within the plane of densest Brn3a label and in axons within the plane of densest SMI32 label. We also quantified at higher magnification (180×) NaV1.6 in confocal stacks through SMI32-labeled varicosities in the proximal axon segment adjoining the RGC body.

Colocalization Analysis. Vertical frozen sections from saline ($n = 6$), 2-wk ($n = 3$), and 4-wk ($n = 3$) microbead retinas were simultaneously immunolabeled for PSD95 and RIBEYE (as described above). Two 200× confocal images (Fluoview 1000) of randomly selected inner plexiform layer areas per condition were acquired. We assessed colocalization between PSD95 and RIBEYE using the Coloc2 plugin within ImageJ software. The intensity threshold of each image was calculated, and we assessed the percentage of colocalization between PSD95 and RIBEYE (tM1) and the percentage of colocalization of RIBEYE to PSD95 (tM2) (2).

Measuring Inhibitory Currents. To investigate light-evoked inhibitory currents, using the same 365-nm light stimulus as described in the main text, we performed voltage-clamp recordings ($V_c = +10$ mV) from RGCs in whole-mount retinas. Pipettes contained (in mM) 105 $CsMeSO_3$, 6 tetraethylammonium-Cl, 20 Hepes, 10 EGTA, 5 Mg-ATP, 0.5 Tris-GTP, 2 QX314-Cl, 0.1 Spermine, and 0.1 Alexa 555 (pH 7.3, Osm = 280, pipette resistance 5–7 MΩ). RGC type was verified by light response profiles in real time and later confirmed by recovering RGC dendritic stratification within the inner plexiform layer and SMI32 labeling using confocal microscopy as described.

SI Results

Pruning of αOFF-T RGC Dendritic Arbors. The dendritic arbors of αOFF-T RGCs demonstrated dramatically reduced size and complexity following 2 wk of elevated IOP, which was significant by Sholl analysis within a radius of 130–240 μm from the soma (Fig. S4*C*). This change corresponded to a significant reduction in average dendritic field area (33%) and total dendrite length (23%) compared with control at 2 wk ($P \leq 0.05$; Fig. S4*D*). Once again, although dendritic complexity, field area, and total length remained significantly diminished ($P \leq 0.02$), pruning did not progress between 2 and 4 wk of elevation.

Pruning in the DBA/2J Mouse. Our results from the inducible model indicate both ON and OFF dendritic arbors are susceptible to pruning. To test this more broadly, we quantified RGC dendritic complexity in DBA/2J mice. For dye-filled DBA/2J RGCs classified as ON, OFF, or ON-OFF based on dendritic stratification (Fig. S5*A*), we noted significant reductions in dendritic complexity in retinas from aged animals (10 mo) compared with naïve C57 (Fig. S5 *B* and *C*). When quantified using Sholl analysis, for young (3 mo) DBA/2J retina, only ON RGCs demonstrated a modest reduction in complexity, and then only close to the cell body (Fig. S6*A*). Interestingly, these same cells showed slightly more dendritic complexity at midrange distances compared with C57. By 10 mo, all RGCs had reduced dendritic field complexity and area and diminished total dendrite length and branch points (Fig. S6). Thus, dendritic pruning in both inducible and chronic models affects ON and OFF arbors alike.

AMPA-Mediated Responses. We isolated pharmacologically the influence of excitatory AMPA receptor signaling in RGCs by silencing other glutamatergic receptors, voltage-gated sodium channels, and inhibitory currents (3) (Fig. S7). Under these conditions, αON-S RGCs failed to demonstrate an enhanced response to light onset; indeed, the AMPA-mediated response integrated over the duration of the light stimulus did not change at all with elevated IOP ($P = 0.75$; Fig. S7*B*). We obtained a similar result for αOFF-S RGCs ($P = 0.16$; Fig. S7 *C* and *D*). For ON-OFF RGCs, the AMPA-mediated light response did not differ from control after 2 wk of elevated IOP for either the ON or OFF component ($P \geq 0.38$; Fig. S7 *C* and *D*). However, by 4 wk, both components significantly declined compared with control ($P \leq 0.03$). Similarly, the response for αOFF-T RGCs did not change after 2 wk ($P = 0.22$), but did diminish by four ($P = 0.05$; Fig. S7 *C* and *D*). Finally, we tested the response of αON-S and ON-OFF RGCs to AMPA delivered directly to the cell by puff pipette (Fig. S7*E*). This measurement reflects the activity of postsynaptic AMPA receptors (4). The response to AMPA for both RGC types decreased progressively between 2 and 4 wk of IOP elevation, with the integrated current response reaching a significant reduction by 4 wk (Fig. S7*F*).

Excitatory Glutamatergic Signaling Components. Localization of PSD95, which stabilizes the glutamatergic postsynaptic density on RGC dendrites (5, 6), remained near control levels in the inner plexiform layer after 2 wk of elevated IOP (Fig. S8 *A* and *B*). However, by 4 wk of elevated IOP, PSD95 levels diminished significantly in the inner plexiform layer compared with control ($P = 0.003$). PSD95 did not change in the outer retina for either time ($P \geq 0.12$), nor did it differ between the ON and OFF sublaminas ($P \geq 0.09$). Surprisingly, we found that 2 wk of elevated pressure increased the presynaptic ribbon marker RIBEYE by twofold in the inner plexiform layer compared with control ($P = 0.04$); by 4 wk, label returned to control levels ($P = 0.14$; Fig. S8 *C* and *D*). Label for RIBEYE did not differ between the ON and OFF sublaminas for either 2 or 4 wk of elevated pressure ($P \geq 0.08$), nor did levels change in the outer retina where photoreceptor axon terminals ramify ($P \geq 0.15$). Even as RIBYEYE increased, colocalization with PSD95 did not change for either IOP exposure compared with control retina ($P \geq 0.47$; Fig. S8 *E* and *F*).

Inhibitory Currents Do Not Change. We recorded from αON-S RGCs under pharmacological and voltage parameters that isolate chloride-driven inhibitory currents (3). Under these conditions, αON-S RGCs demonstrate a sustained outward current in response to light due to chloride influx that was similar between control and 2-wk cells (Fig. S8*G*). When quantified across cells, the chloride-driven inhibitory current did not differ between control and 2-wk αON-S RGCs ($P = 0.5$; Fig. S8*H*). We found a similar result for several OFF RGCs ($P \geq 0.48$). The minor reduction in response we do see at 2 wk is consistent with early changes in GABAergic signaling observed in other glaucoma models (7, 8).

1. Weitlauf C, et al. (2014) Short-term increases in transient receptor potential vanilloid-1 mediate stress-induced enhancement of neuronal excitation. *J Neurosci* 34: 15369–15381.
2. Manders EMM, Verbeek FJ, Aten JA (1993) Measurement of co-localization of objects in dual-colour confocal images. *J Microsc* 169:375–382.
3. Sullivan SJ, Miller RF (2012) AMPA receptor-dependent, light-evoked D-serine release acts on retinal ganglion cell NMDA receptors. *J Neurophysiol* 108:1044–1051.
4. Cohen ED (2000) Light-evoked excitatory synaptic currents of x-type retinal ganglion cells. *J Neurophys* 83:3217–3229.
5. Euler T, Haverkamp S, Schubert T, Baden T (2014) Retinal bipolar cells: Elementary building blocks of vision. *Nat Rev Neurosci* 15:507–519.
6. Morgan JL, Schubert T, Wong RO (2008) Developmental patterning of glutamatergic synapses onto retinal ganglion cells. *Neural Dev* 3:8.
7. Moon JI, et al. (2005) Changes in retinal neuronal populations in the DBA/2J mouse. *Cell Tissue Res* 320:51–59.
8. Zhou X, et al. (2017) Alpha7 nicotinic acetylcholine receptor agonist promotes retinal ganglion cell function via modulating GABAergic presynaptic activity in a chronic glaucomatous model. *Sci Rep* 7:1734.

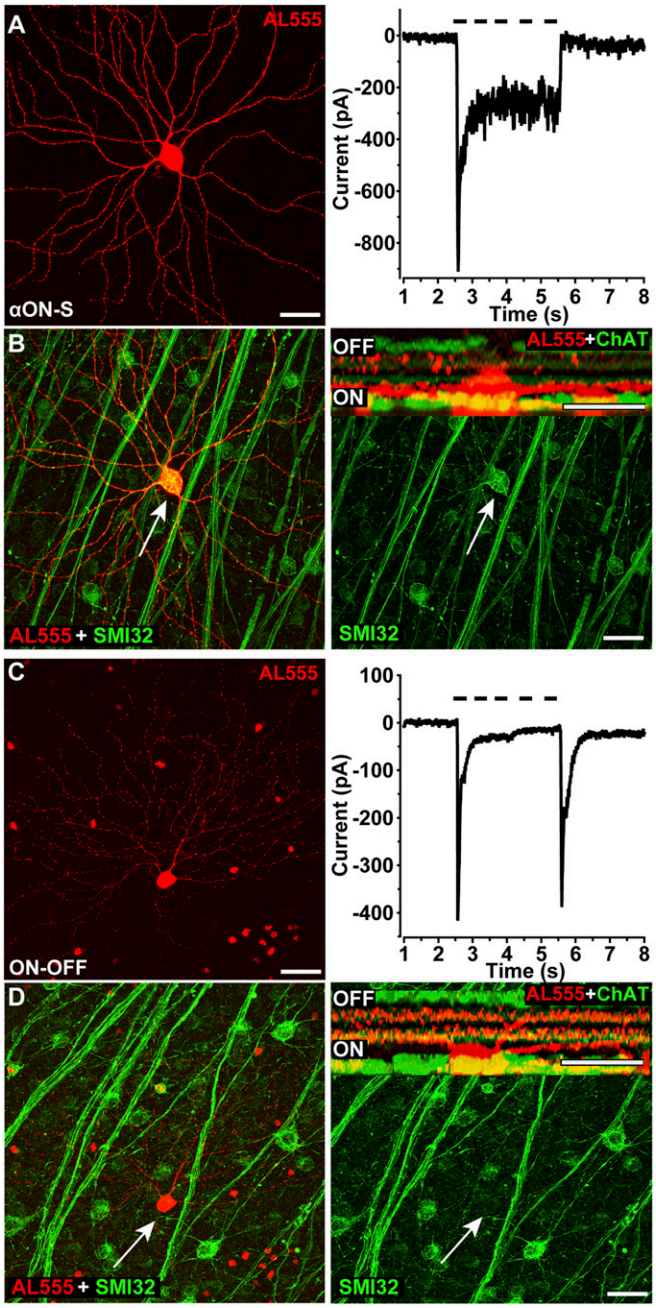

Fig. S1. Classification of αON-sustained and ON-OFF RGCs. (*A*, *Left*) Confocal micrograph of αON-sustained (αON-S) RGC (control retina) following intracellular filling with Alexa 555 dye (AL555). (*A*, *Right*) Current response to light stimulus (dashed line) over time in seconds under voltage clamp (−65 mV) conditions for the same RGC. This type shows a large, brief transient inward (depolarizing) current followed by a sustained component for the duration of the stimulus, consistent with published recordings (1, 2). (*B*) AL555-filled αON-S RGC (red) strongly expresses nonphosphorylated neurofilament H protein (SMI32, green). (*Inset*) Orthogonal rotation shows dendrites ramifying narrowly in the ON sublamina relative to label for choline acetyltransferase (ChAT, green). (*C*, *Left*) ON-OFF RGC from CTRL retina following AL555 filling. (*C*, *Right*) This ON-OFF type shows transient inward current to both light onset and offset as in other published recordings (3, 4). (*D*) AL555-filled ON-OFF RGC (red) has negligible immunolabeling for SMI32 (green). (*Inset*) Orthogonal rotation shows dual dendritic arbors in both ON and OFF sublaminas, shown with ChAT label (green) for reference. (Scale bar: 40 μm.)

1. Pang JJ, Gao F, Wu SM (2003) Light-evoked excitatory and inhibitory synaptic inputs to ON and OFF alpha ganglion cells in the mouse retina. *J Neurosci* 23:6063–6073.
2. van Wyk M, Wässle H, Taylor WR (2009) Receptive field properties of ON- and OFF-ganglion cells in the mouse retina. *Vis Neurosci* 26:297–308.
3. Trenholm S, Johnson K, Li X, Smith RG, Awatramani GB (2011) Parallel mechanisms encode direction in the retina. *Neuron* 71:683–694.
4. Yoshida K, et al. (2001) A key role of starburst amacrine cells in originating retinal directional selectivity and optokinetic eye movement. *Neuron* 30:771–780.

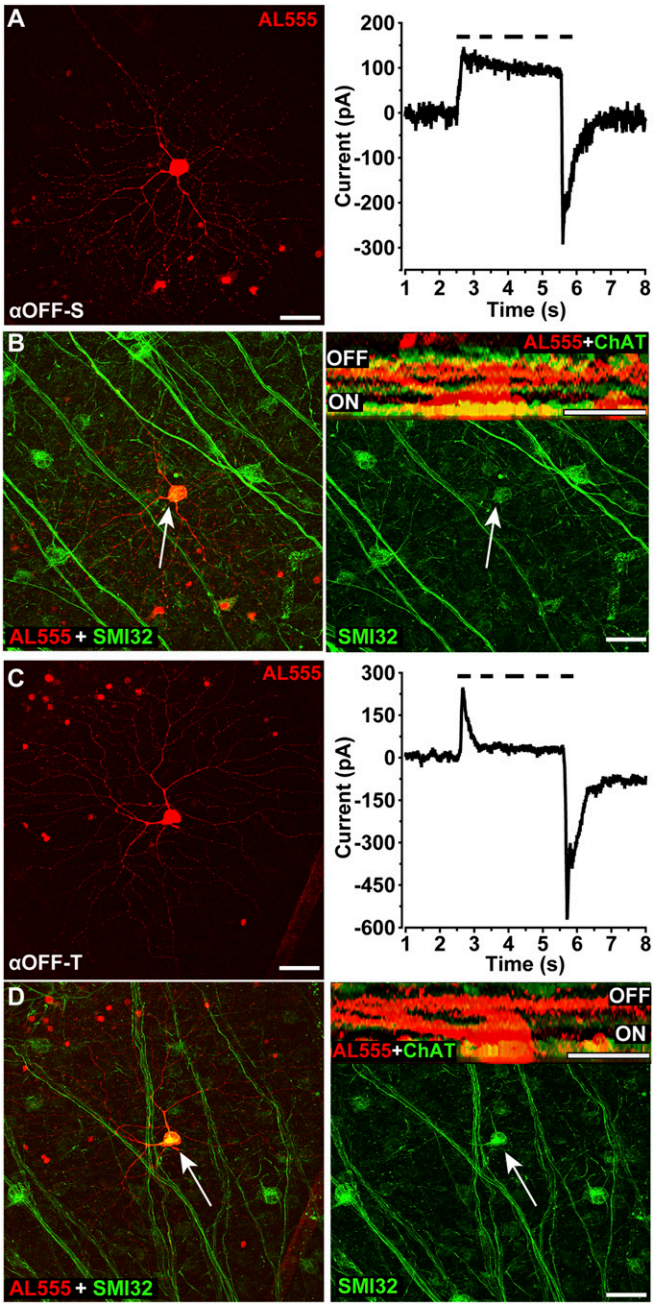

Fig. S2. Classification of αOFF RGCs. (*A*, *Left*) Confocal micrograph of αOFF-S RGC (control retina) following intracellular filling (AL555). (*A*, *Right*) Current response to light stimulus (dashed line) over time in seconds under voltage clamp (−65 mV) conditions. The αOFF-S type shows sustained outward current during the stimulus and inward current at light offset, as in other published recordings (1, 2). (*B*) AL555-filled αOFF-S RGC (red) also expresses SMI32 (green). (*Inset*) Orthogonal rotation shows stratification in the OFF sublamina, highlighted by ChAT label (green) for reference. (*C*, *Left*) αOFF-T RGC from CTRL retina following AL555 filling. (*C*, *Right*) Current response to light shows transient inward current at light offset and smaller transient outward current at onset, consistent with published recordings (1). (*D*) αOFF-T RGCs strongly express SMI32 with dendrites ramifying narrowly in the OFF sublamina relative to ChAT (*Inset*). (Scale bars: 40 μm.)

1. Pang JJ, Gao F, Wu SM (2003) Light-evoked excitatory and inhibitory synaptic inputs to ON and OFF alpha ganglion cells in the mouse retina. *J Neurosci* 23:6063–6073.

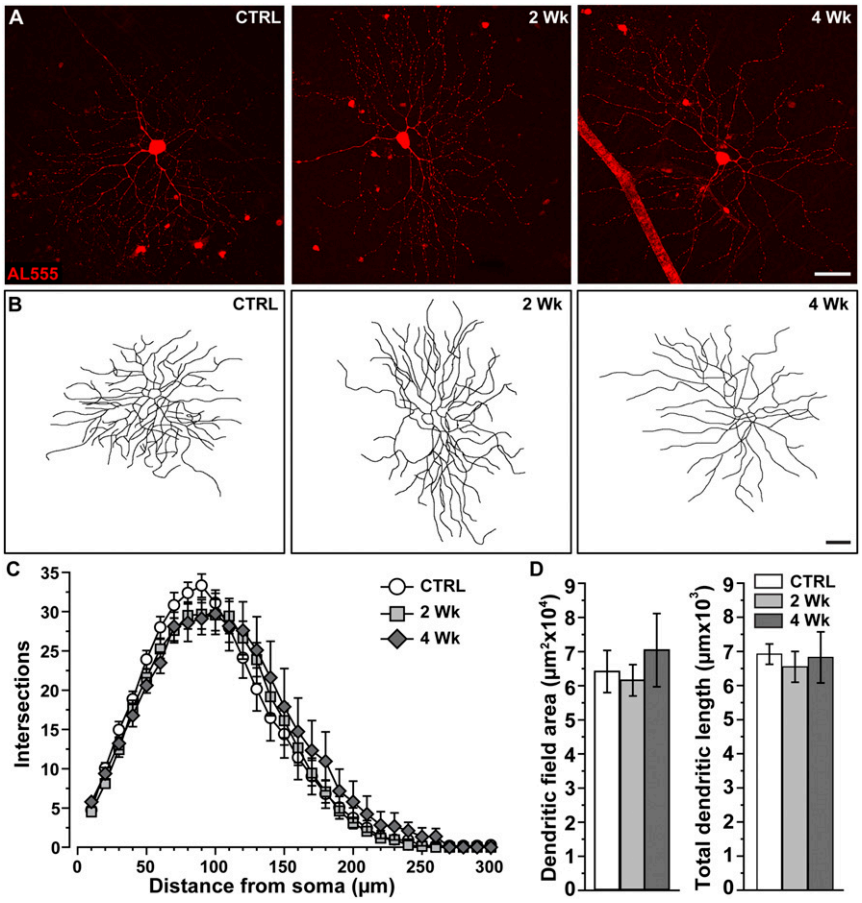

Fig. S3. αOFF-S RGCs are less vulnerable to dendritic pruning than αON-S. (*A*) Examples of αOFF-S RGCs from CTRL, 2-wk, and 4-wk retinas. (*B*) Reconstructions of αOFF-S RGCs show little change in dendritic arborization with elevated IOP. (Scale bars: *A* and *B*, 40 μm.) (*C*) Sholl analysis shows no change in complexity for either 2-wk ($n = 15$) or 4-wk ($n = 7$) αOFF-S RGCs compared with CTRL ($n = 12$). $P = 0.68$, two-way ANOVA. (*D*) Elevated IOP does not significantly affect dendritic field area and length for either 2-wk or 4-wk groups ($P \geq 0.52$, *t* tests). Data: mean ± SEM.

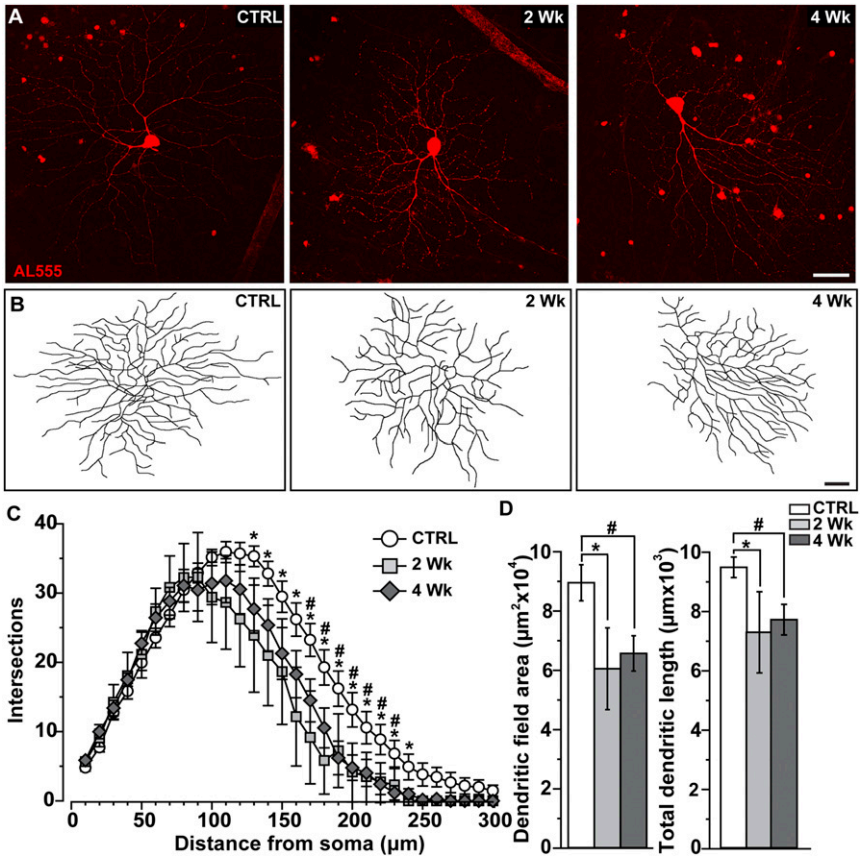

Fig. S4. Dendritic pruning is not confined to the ON sublamina. (*A*) αOFF-T RGCs from CTRL, 2-wk, and 4-wk retinas following intracellular filling (AL555). (*B*) Reconstructions of αOFF-T cells show reduced arborization with elevated IOP. (Scale bars: *A* and *B*, 40 μm.) (*C*) Sholl analysis averaged across αOFF-T RGCs shows reduced complexity from 130 to 240 μm for 2-wk cells ($n = 7$) compared with CTRL ($n = 14$; $^{*}P \leq 0.03$, two-way ANOVA) and from 170 to 230 μm for 4-wk cells ($n = 10$; $^{\#}P \leq 0.03$). (*D*) Dendritic field area decreases for both 2- and 4-wk groups compared with control (*, $^{\#}P \leq 0.05$), as does total dendrite length (*, $^{\#}P \leq 0.03$). Data: mean ± SEM.

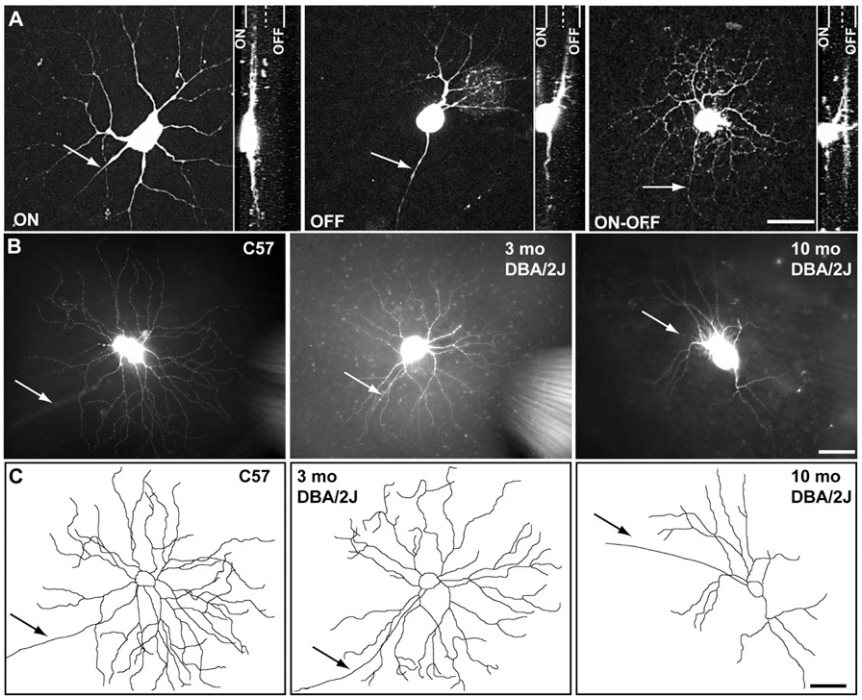

Fig. S5. Assessing dendritic pruning in a chronic model. (*A*) Examples of dye-filled ON, OFF, and ON-OFF RGCs following intracellular injection in C57 retina with their respective orthogonal rotations to illustrate stratification (*Insets*). (*B*) Maximum projection micrographs of ON RGCs in C57, 3-mo, and 10-mo DBA/2J mice; axon (arrow) remains intact for each. (*C*) Reconstructions of same RGCs with axons (arrows) illustrate significant dendritic pruning in 10-mo DBA/2J. (Scale: 30 μm.)

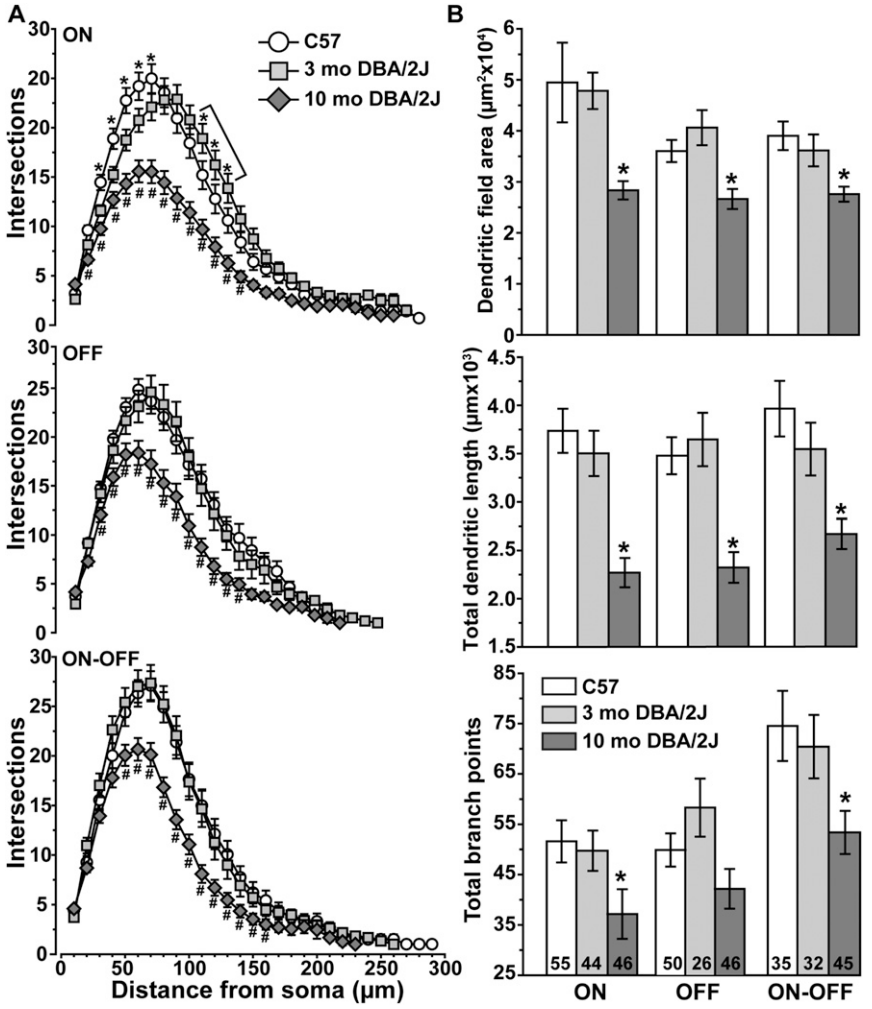

Fig. S6. Dendritic pruning in a chronic model is independent of ON and OFF. (*A*) Sholl analysis averaged across ON (*Top*), OFF (*Middle*), and ON-OFF (*Bottom*) RGCs shows significant decrease in dendritic intersections in 10-mo DBA/2J compared with C57 at most distances from soma ($^{\#}P \leq 0.05$, two-way ANOVAs). For 3-mo-old retinas, only ON RGCs showed modest loss of complexity in dendrites proximal to the soma compared with C57 ($^{*}P \leq 0.02$, two-way ANOVA). However, these cells also demonstrated slightly more complexity at midrange distances from the soma (bracketed $^{*}P \leq 0.05$, two-way ANOVA). (*B*) For 10-mo DBA/2J retina, ON and ON-OFF RGCs all demonstrate significant reductions (*) in dendritic field area (*Top*; $P \leq 0.01$, one-way ANOVAs), total dendrite length (*Middle*, $P \leq 0.001$, one-way ANOVAs), and total number of branch points (*Bottom*, $P \leq 0.04$, one-way ANOVAs). For 10-mo OFF RGCs, the decrease in total branch points was not significant ($P = 0.3$, one-way ANOVA). *Inset* indicates numbers of RGCs in each mouse group for the three classes of cells. Data: mean ± SEM.

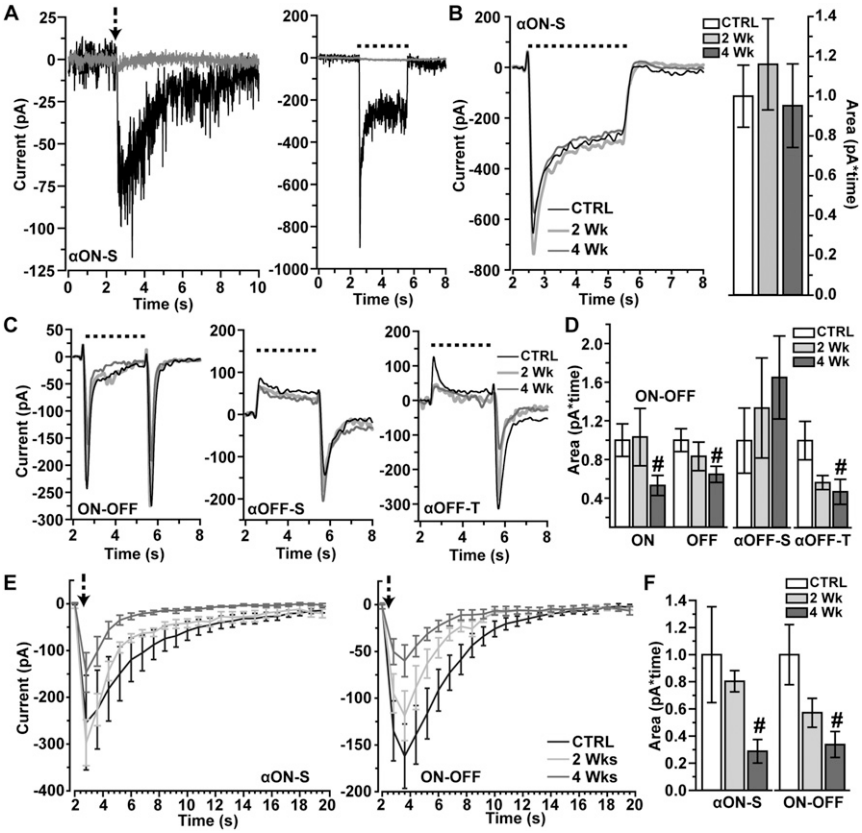

Fig. S7. Enhanced RGC light response is not mediated by AMPA receptor signaling. (*A*) Voltage-clamped (−65 mV) current responses of a control αON-S RGC to a 20-ms puff of AMPA (*Left*, arrow) or a 3-s pulse of light (*Right*, dashed line) before (black traces) and after (gray traces) bath application of 100 μM CNQX to block AMPA receptor activation. The bath also contained TTX, PTX, strychnine, and AP5 to block, respectively, voltage-gated sodium channels, $GABA_A$ receptors, glycine receptors, and NMDA receptors. After addition of CNQX, inward currents evoked by either AMPA or light are eradicated, consistent with the known role for AMPA receptors in mediating glutamatergic excitation in RGCs (1, 2). (*B*, *Left*) AMPA receptor-mediated current responses to 3-s light stimulus (dashed line) averaged for CTRL ($n = 3$), 2-wk ($n = 4$), and 4-wk ($n = 5$) αON-S RGCs under voltage clamp to prevent chloride-driven inhibitory currents (−65 mV). (*B*, *Right*) Average AMPA-mediated response for αON-S RGCs integrated over the duration of the light stimulus did not differ between groups ($P = 0.75$). (*C*, *Left*) AMPA receptor-mediated current responses to light stimulus (dashed line) under voltage clamp (−65 mV) averaged from CTRL ($n = 6$), 2-wk ($n = 5$), and 4-wk ($n = 7$) ON–OFF RGCs. (*C*, *Center*) Same responses for CTRL ($n = 8$), 2-wk ($n = 9$), and 4-wk ($n = 9$) αOFF-S RGCs. (*C*, *Right*) Same conditions for CTRL ($n = 4$), 2-wk ($n = 10$), and 4-wk ($n = 11$) αOFF-T RGCs. (*D*) Average integrated AMPA-mediated response for ON-OFF, αOFF-S, and αOFF-T RGCs. ON component for ON-OFF RGCs integrated over the duration of the light stimulus; OFF component and responses for αOFF-S, and αOFF-T RGCs integrated for 3-s period following light offset. The response for αOFF-S RGCs did not change with elevated IOP ($P = 0.16$). Whereas 2 wk of elevation had no effect for ON-OFF, αOFF-S, and αOFF-T RGCs ($P \geq 0.22$), 4 wk diminished each response significantly ($^{\#}P \leq 0.05$). (*E*) Average voltage-clamped (−65 mV) current responses from CTRL, 2-wk, and 4-wk αON-S (*Left*) and ON-OFF (*Right*) RGCs evoked through direction administration of 100 μM AMPA (arrow) to the cell body. (*F*) Average integrated current response to direct application of AMPA for CTRL ($n = 12$), 2-wk ($n = 12$), and 4-wk ($n = 11$) αON-S RGCs and for CTRL ($n = 12$), 2-wk ($n = 13$), and 4-wk ($n = 4$) ON-OFF RGCs. AMPA-induced currents decrease at 2 wk and become significantly lower than control by 4 wk ($^{\#}P \leq 0.05$). Data: mean ± SEM.

1. Kalbaugh TL, Zhang J, Diamond JS (2009) Coagonist release modulates NMDA receptor subtype contributions at synaptic inputs to retinal ganglion cells. *J Neurosci* 29:1469–1479.
2. Sullivan SJ, Miller RF (2012) AMPA receptor-dependent, light-evoked D-serine release acts on retinal ganglion cell NMDA receptors. *J Neurophysiol* 108:1044–1051.

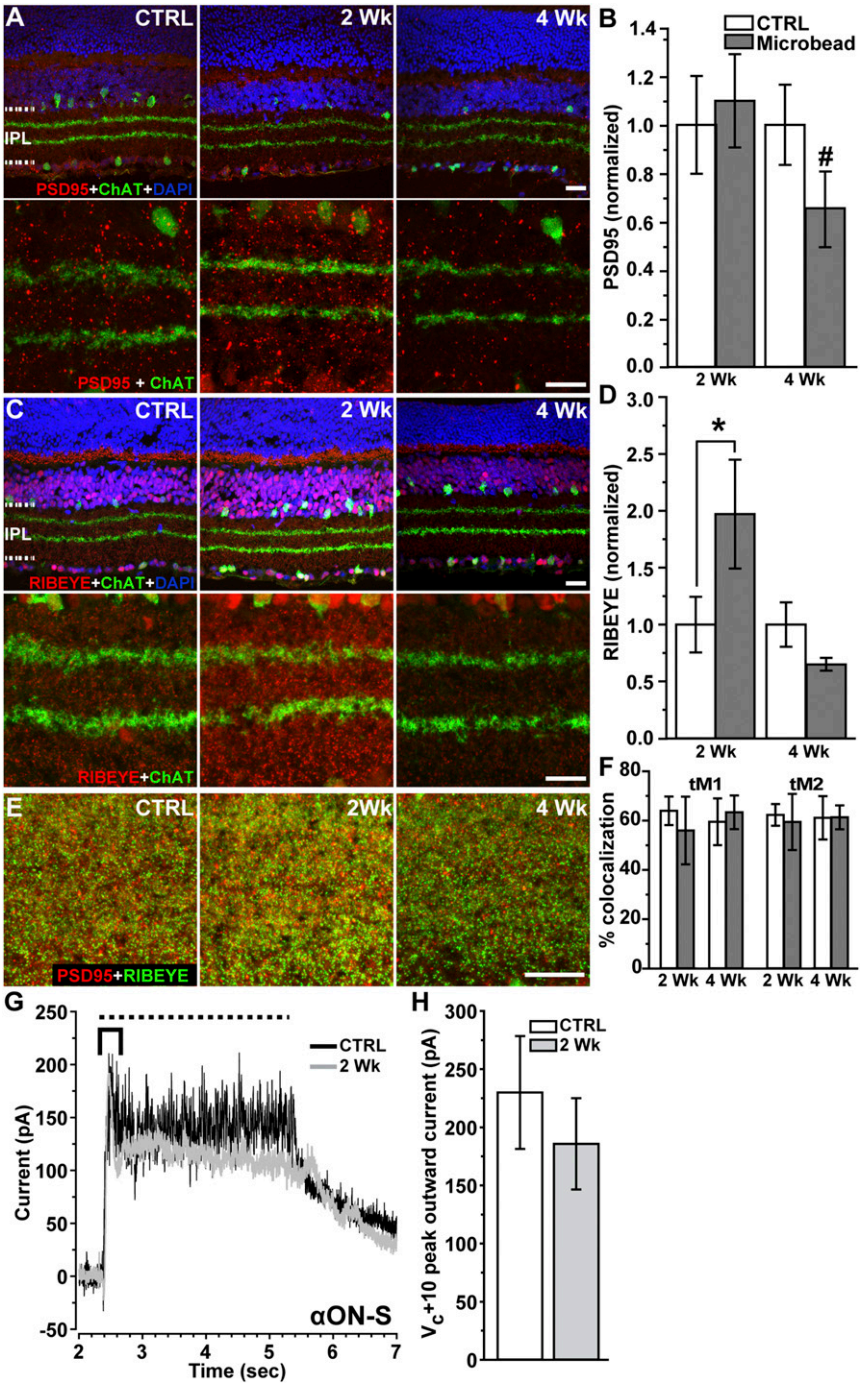

Fig. S8. IOP-induced changes in glutamatergic signaling components. (*A*) Confocal micrographs of vertical sections from CTRL, 2-wk, and 4-wk retinas labeled for the postsynaptic density protein PSD95 and ChAT and counterstained with the nuclear dye DAPI for reference. Higher magnification of inner plexiform layer (IPL, *Lower*) shows decrease in PSD95 in 4-wk retina. (*B*) Mean levels of PSD95 relative to ChAT and normalized with respect to CTRL ($n = 8$) retina do not change in 2-wk ($n = 8$) retina ($P = 0.64$), but diminish in 4-wk ($n = 6$) retina ($^{\#}P = 0.003$). (*C*) Label for the presynaptic ribbon protein RIBEYE relative to ChAT and DAPI for reference. Higher magnification of IPL (*Lower*) shows increase in RIBEYE for 2-wk retina. (*D*) Mean levels of RIBEYE relative to ChAT and normalized to CTRL retina increased after 2 wk ($P = 0.04$), but returned to CTRL levels by 4 wk ($P = 0.14$). Sample numbers same as for PSD95. (*E*) High-magnification confocal micrographs of IPL colabeled for PSD95 and RIBEYE show little change in colocalization with elevated IOP. (*F*) Percent colocalization of PSD95 with RIBEYE (tM1) and of RIBEYE with PSD95 (tM2) do not change with either 2 wk ($n = 3$ retina) or 4 wk ($n = 3$) of elevated IOP compared with CTRL ($n = 3$) retina ($P \geq 0.47$). (*G*) Current responses of CTRL and 2-wk αON-S RGCs to a 3-s pulse of light (dashed line) under voltage clamp near cation channel equilibrium (+10 mV) to isolate inhibitory chloride currents. Cells demonstrate sustained outward current with similar peaks (bracket) due to chloride influx (1) (*Methods*). (*H*) Average light-induced peak outward (inhibitory) current due to chloride is similar for CTRL ($n = 2$) and 2-wk ($n = 3$) αON-S RGCs ($P = 0.5$). (Scale bars: *A*, *C*, and *E*, 20 μm.) Data: mean ± SEM.

1. Pang JJ, Gao F, Wu SM (2003) Light-evoked excitatory and inhibitory synaptic inputs to ON and OFF alpha ganglion cells in the mouse retina. *J Neurosci* 23:6063–6073.

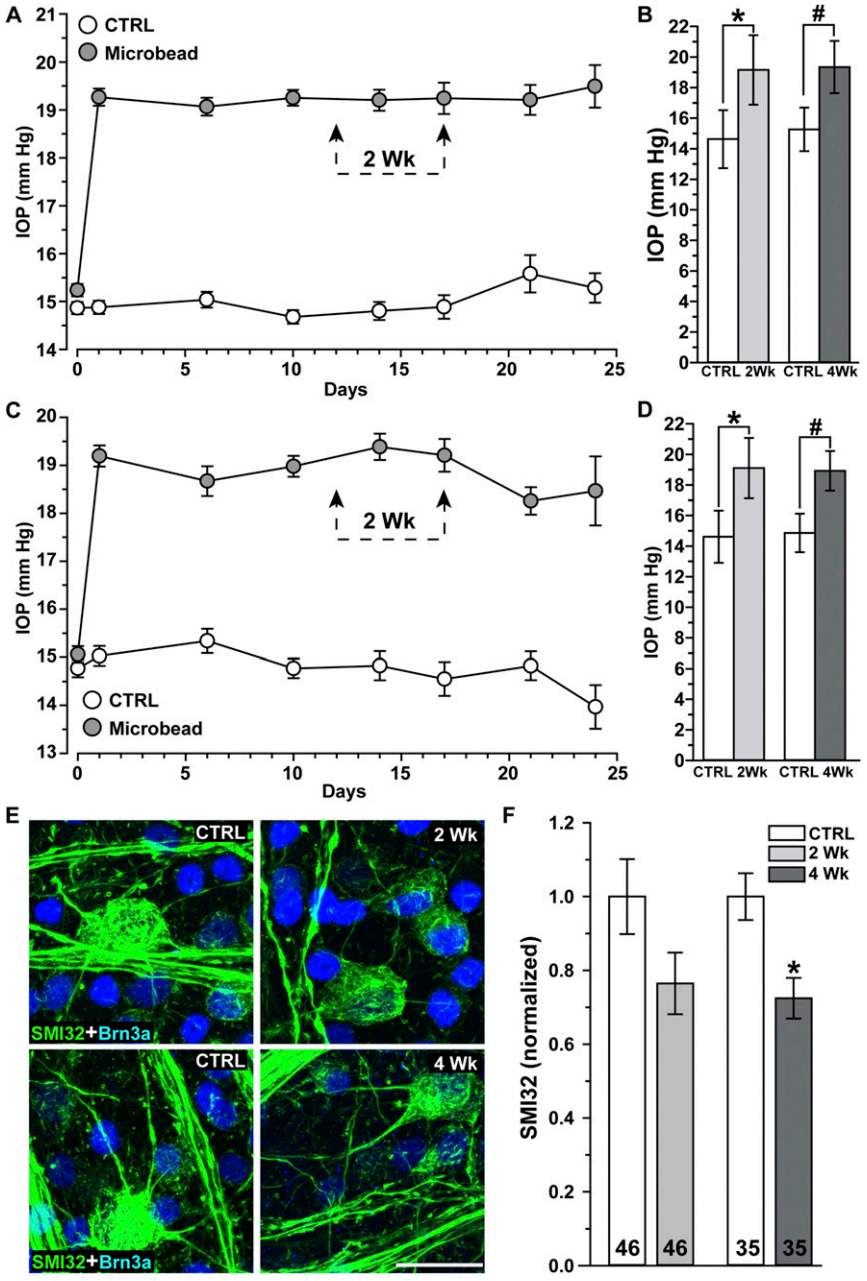

Fig. S9. Elevated ocular pressure in mice. (*A*) IOP in units of mmHg (mean ± SE) for C57 mouse eyes before (day 0) and following (days ≥ 1) a single unilateral injection of polystyrene microbeads (1.5 μL) or equivalent volume of saline (CTRL). For physiological recordings and morphological analysis, a 2-wk cohort was killed between 12 and 16 d postinjection (dashed arrows; $n = 32$ animals), and a 4-wk cohort ($n = 14$ animals) was killed 26–30 d postinjection. (*B*) Microbeads caused a significant increase in mean IOP postinjection compared with CTRL eyes for both 2-wk (19.2 ± 2.3 vs.14.6 ± 1.9 mmHg; $^{*}P < 0.001$) and 4-wk (19.3 ± 1.7 vs.15.3 ± 1.4, $^{\#}P < 0.001$) cohorts. (*C*) IOP for CTRL ($n = 16$) and microbead ($n = 16$) C57 eyes used for immunolabeling and axonal anterograde transport studies (Fig. 6 *A* and *B*) showed same trend as physiological cohort. (*D*) Microbead eyes showed significant IOP increase compared with CTRL for both 2-wk (19.1 ± 2.0 vs.14.6 ± 1.7 mmHg; $^{*}P < 0.001$) and 4-wk (19.0 ± 1.3 vs.14.9 ± 1.3, $^{\#}P < 0.001$) cohorts. (*E*) Confocal micrographs through ganglion cell layer of CTRL, 2-wk, and 4-wk retinas labeled for SMI32 and the RGC marker Brn3a. (Scale bar: 40 μm.) (*F*) Mean levels of SMI32 normalized with respect to CTRL retina do not change in 2-wk retina ($P = 0.12$), but diminish in 4 wk ($^{\#}P = 0.001$). Even so, SMI32+ RGCs remain easily distinguished. Number of cells analyzed indicated for each. Data: mean ± SEM.